Process analysis on milled optical surfaces in hardened stainless steel

M. Groeb, M. Fritz
Kern Microtechnik GmbH, Germany

Abstract

The capability to produce surfaces in optical quality is of rising prominence in the manufacturing industry. The die and mould industry have to meet rising requirements, in regard to surface finish and geometric precision, to keep pace with technological advances in sectors such as illumination, optical sensors as well as fibre technology. Historically moulds were either produced by hand polishing, an expensive process where the achieved finish and accuracy is largely dependent on the experience of the worker. Alternatively, injection moulds have been produced in non-ferric materials by costly diamond milling, with a further drawback in form of a limited lifetime compared to steel moulds. This paper focuses on the challenges in developing a sample milling process for optical surface finishes in 53 HRC STAVAX stainless steel. Besides the expected process and tooling parameter variations, three prominent material analytics methods were used to evaluate all experiments. The tool wear was analysed and monitored via SEM and EDS. To verify the milling process capabilities, a sample was produced through manual polishing and then analysed for material faults via nanoindentation and BSE analysis. The finished results were measured for their surface roughness via bifocal laser microscopy and for their topography SEM. In the practical application, a surface roughness R_a in the single digit nm range was achieved.

1 Introduction

The capability to produce surfaces in optical quality is of rising prominence in the manufacturing industry. Sectors such as illumination, optical sensors, fibre technology but also die and mould demand milled surfaces in the highest possible quality, whereas the need for automation and man less production require a finished part right off the machine. The global injection moulded plastic market has been valued at several hundred billion dollars in 2016 [1]. Consequently, research is being carried out into improving milled surfaces, with the arithmetical surface roughness R_a as the most often used quality parameter. The limiting factor of the achievable surface roughness is not only the machine, but a broader range of parameters, including but not limited to process, tool, material and cutting conditions [2]. Furthermore, nanoscale surfaces set rising requirements to the measuring and evaluation technique in quality control. The Society of the Plastics Industry (SPI) has set a standard for injection moulding, where the highest achievable finish is grade A-1 with a typical surface roughness R_a between 0.012 and 0.025 µm [3]. A surface roughness in the single digit nanometre range is desired. Traditionally, the injection mould is manufactured through several steps. First, the general shape of the part is roughed out on a milling machine, followed by a heat treatment to increase the durability of the mould. The desired shape is created through electrical discharge machining (EDM), an expensive and complex process requiring the creation of an electrode beforehand. Afterwards, the form is polished manually in a labour-intensive process, which is largely dependent on the skill and experience of the worker. Shorter time to market, a general shortage of skilled employees as well as the advancing automation require a new approach. Contrarily to the traditional use of EDM to create small features, the use of high-speed spindles enables productive application of small tooling. The desired surface quality is achievable through special coated tools or diamond cutting directly on the milling machine. Summarily, the limitations of the traditional production for injection moulds, milling requires specialized tooling, a capable machine and a fine control over the process. In this paper, the process for creating high quality surfaces in hardened stainless steel via a polycrystalline diamond tool is explored. For this, the material is analysed with a confocal laser microscope in regard to the surface roughness. A scanning electron microscope (SEM) is used to determine the topography, energy dispersive x-ray spectroscopy (EDS) for the elemental analysis of material anisotropies as well as the wear of the tooling used. Nano indentation verifies the material isotropy as well as specimen hardness. Several specimen are produced under varying cutting conditions.

2 Process and surface faults

This paper focuses on the application of free-form milling regarding the surface finish. This finish is primarily dependent on the machine, cutting conditions, tool geometry, the environmental conditions, material property, chip formation as well as vibration [2]. The surface topography is formed as a result of the tool

- workpiece interaction, therefore the material removal mechanism is of greater importance [2]. Figure 1 shows the four dominant chip formation mechanisms in milling.

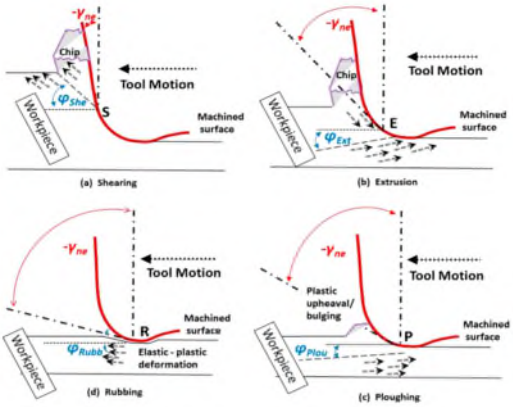

Figure 1: The four distinct chip formation mechanisms in milling. From [2]

While the shearing and extrusion process are dominant in normal machining, in precision machining (PM) the rubbing and ploughing mechanism (figure 2.1 c, d) are predominate [7]. Furthermore, the ratio of the undeformed chip thickness to the tool edge radius (relative tool sharpness, RTS) is the defining parameter of the theoretically achievable surface roughness in milling processes [7], [2].

In high-precision machining, the surface roughness can be in the same range as the uncut chip thickness [8]. The theoretically achievable surface roughness (see fig. 2) is a function of the tool radius (r) as well as the axial runout (a), which can be calculated through equation 1 [9]. F_z is the feed per tooth.

$$R_{th} = \frac{F_z^2}{8r} + a \tag{1}$$

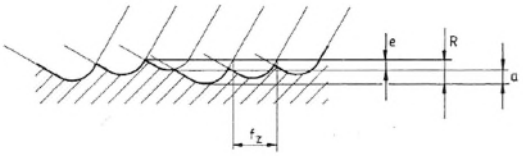

Figure 2: Kinematic roughness. F_z is the feed per tooth, R the resulting roughness, whereas the resulting deviation from the ideal line is specified by e and a. (from [8])

While the surface may have a good macroscopic appearance, small surface defects appear on the milled surface. These surface faults originate from the difference between micro and macroscale cutting. This results from the so called

'size effect', meaning the increase in material shear flow stress as the chip thickness decreases. Because the fault size is so small, SEM observation is necessary. Figure 3 shows the major surface faults along the cutting plane.

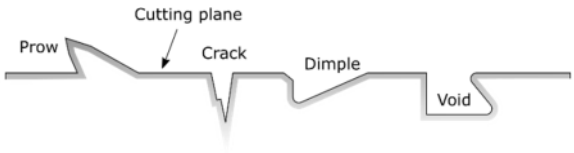

Figure 3: Surface faults in micro-milling

In the previously used process by Kern, a polycrystalline diamond (PCD) coated radius ball mill was used with an ISO-strategy to finish the surface. The optical surface has a high visible gloss and a surface roughness R_a = 0.015 µm. Visible surface faults are grooves along the feed direction, generally very fine scratches in every orientation as well as an inconsistent gloss.

Figure 4: Milled optical surface

3 Experimental Investigations

The material used in all experiments is Stavax ESR (electro slag remelting), produced by Uddeholm GmbH. The delivered specimens have a size of 30 x 23 x 102 mm. The material is delivered in an annealed state and cut by saw. The smelter number of the batch used is A16002. Before hardening, the material is roughed out to create square and comparable specimen. A drafted surface with an inclination of 45° is milled to enable 3 axis milling at a sensible point of engagement with the radius tooling used. The roughed out material is cleaned with ethanol alcohol in an ultrasonic cleaner. Hardening is done with the Uddeholm proposed process. A hardness of 53 HRC +/- 1 HRC was achieved.

In order to examine the bulk material used for anisotropies, a hardened sample is prepared with a hand polishing process. For this, the sample is first ground on a rotary grinding machine (Metko Gripo 2) with increasingly finer grit (from 80 to 4000 in 10 steps). The grinding direction on the sample is rotated for 90 degrees before the next step and the grinding process is stopped once the grind marks from the previous step are completely removed. Water coolant is used during the grinding process. Following the last grinding step with 4000 grit sandpaper the

sample is cleaned and then polished on a cloth substrate with diamond polishing compound with particles ranging from six micrometer down to one micrometer diameter. An alcohol based wetting fluid is used to reduce the friction. The polished sample is then analysed for its topography in a SEM microscope, followed by nano-indentation. The SEM analysis shows (see figure 5) a uniform surface mildly marred by scratches.

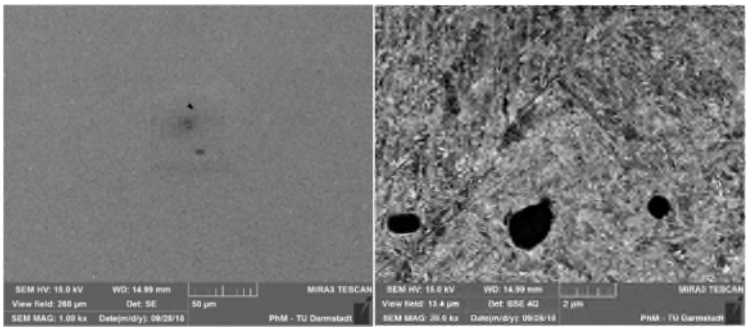

Figure 5: SEM and BSE images of the hand polished sample

Small black dots appear all over the sample, for which the BSE imaging points to an accumulation of lighter elements.

In order to verify that the material is uniform in its behaviour, a nano-indentation test was performed. Both the polished sample as well as an exemplary milled sample are glued to the specimen holder. A matrix of ten by ten indentations is created on every sample. An indentation depth of up to 550 nm was reached.

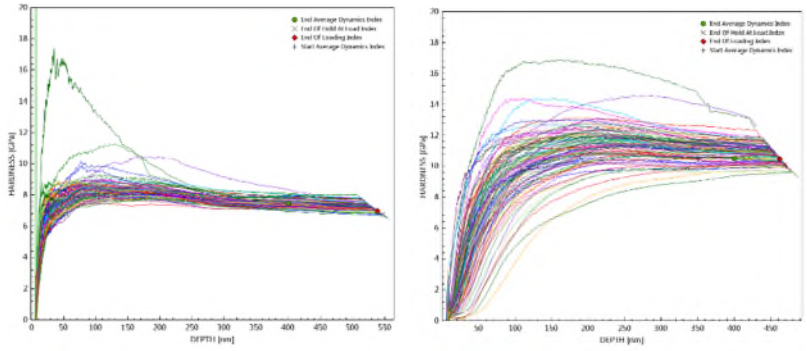

Figure 6: Hardness curves resulting from the nano indentation experiment. Left side: hand polished sample. Right side: milled sample.

In figure 6 it is clearly visible that the hand polished reference sample has a very uniform hardness of about 7,5 GPa. The milled reference sample shows a comparatively deeper hardness plateau, reaching a hardness of up to 11 GPa. The standard deviation on the milled sample is 0,74 GPa, whereas the polished

sample shows a standard deviation of 0,27 GPa. This leads to the conclusion of work hardening of the material during the milling process. A Vickers hardness test with a load of 0,5 kg showed a hardness for the milled sample of on average 670 HV 0,5 (58,9 HRC), further suggesting work hardening of the sample. The polished sample exhibits a very uniform behaviour, making vibrational surface faults arising from anisotropies in the material unlikely.

3.1 Tool analysis

Analysing the tool wear in precision machining is challenging. Because the surfaces are of a very high quality, very small tool wear effects or edge breakouts can have a huge impact. Moreover, a slightly worn or rounded edge is often not visible under optical microscopes, therefore needing higher resolution imaging techniques. A well-established method is the use of a SEM microscope. The SEM is used to both judge wear in a qualitative way, as well as through EDS to make an elemental analysis to detect build up edge phenomena.

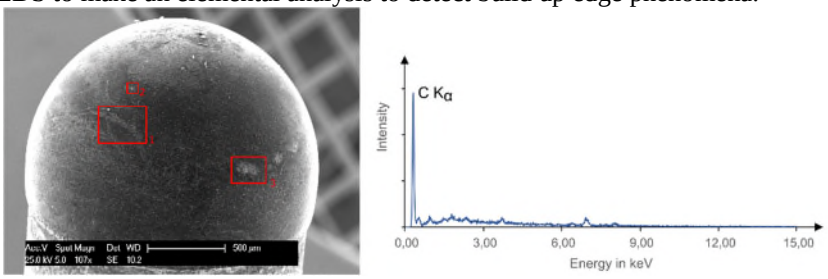

Figure 7: SEM overview of the used tooling as well as the EDS spectra for the undamaged PCD coating.

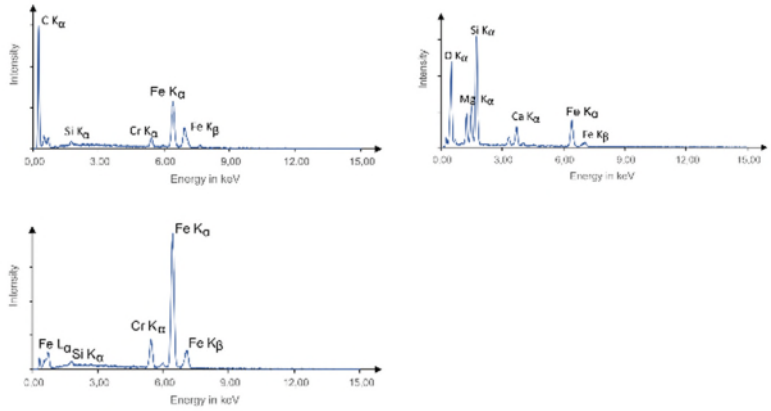

Figure 8: EDS spectra for (from left to right) selections 1-3 from figure 7.

Figure 8 shows the recorded EDS spectra for the used tooling. Section 1 shows a lighter coloured area on the tool. The elemental analysis shows mainly the used specimen material, signifying adherence to the tool. In sections 2 respectively 3, the thicker, unevenly formed particles are analysed. Besides a carbon K alpha peak several iron peaks, silicon as well as chrome are detected. As these are the

elements found in high concentrations in the used stainless steel, the particles on the surface appear to be a chemical adhesion of the work material similar to a build up edge. These particles stuck to the surface of the tool are possibly explaining the occurrence of scratches along the work direction. Conclusively, tool wear is clearly visible after a relatively short period of usage. The most likely wear process here is chemical adherence of the steel to the carbon of the diamond coating.

3.2 Parameter variation

In order to improve on the surface finish, prolonging tool life and avoiding the beforehand mentioned surface faults, a number of process parameter variations were undertaken, mainly adjusting the cutting speed, the feedrate and the depth of cut. The samples were milled with an iso-distribution strategy (meaning the toolpath stepover is evenly distributed along the surface). Table 1 lists the used universal milling parameters, whereas table 2 lists the spindle speed (n) variation and their resulting feed per rotation (f_n) as well as cutting speed (v_c) at 45°. Because the tool has no geometric set cutting edge, the more commonly used feed per tooth cannot be calculated.

Table 1: Universal milling parameters used in the experiments.

A_p (depth of cut)	5 µm
A_e (width of cut)	5 µm
Feedrate	670 mm/min
Coolant	Flood coolant
Milling direction	Climb milling
Dynamics setting	Finishing

Table 2: Cutting speed variation parameters.

n in $kmin^{-1}$	40	37	35	31	28	25	22	19	16	13	10	7	4	3
f_n in µm	19.0	20.5	22.3	24.5	27.1	30.4	34.5	40.0	47.5	58.4	76.6	109	190	253
V_c in m/min	126	116	110	97	88	79	69	60	50	41	31	22	13	9

The feedrate is then gradually reduced from a value of 660 mm/min to 140 mm/min. Because the surface quality in all cutting processes is largely dependent on the force exerted between tool and material, the cutting depth was gradually reduced from 5 µm to 0.5 µm.

3.1 Cleaning Study

Directly after milling the samples are cleaned with compressed air. A black, tough residue is left on the sample. This film appears with refracting colours from different angles. In order to clean milled parts, a common approach is the use of ethanol in an ultrasonic bath. As the residue could not be removed by ethanol, a series of organic solvents and bases were evaluated in their ability to

remove the film. For this, a small drop of the solvent was placed on the sample. After 3 minutes, the drop was wiped away with a precision lab towel and the surface optically examined. Table 3 sums up the results. There, a "-" symbols no visible change, a "o" a small but ineffective change and a "+" a good film removal. It is clearly visible that the organic solvents were unable to remove the film, whereas the best result was obtained with NaOH lye; a concentration of 2M was deemed sufficient. After the application with lye, a cleaning best practice suggests a thorough washing in distilled water followed by spraying the sample with methanol and drying under a hot air fan. A residue free, optical surface was achieved.

Table 3 – Overview of the different cleaning solvents used and their respective effectiveness.

Chemical Substance	**Cleaning result**
Ethanol alcohol	-
Isopropyl alcohol	-
Methanol alcohol	-
Acetone	-
Hexanol	-
Dichloromethane	0
2M NaOH	+
6M NaOH	+

The surface roughness improved from Sa 15 nm to Sa 11 nm, thus highlighting the importance of the cleaning process of optical surfaces.

4 Results

The surface shows a very high gloss uniform over the sample. To the naked eye, there is very little optical variance between the different spindle speed settings. The best surface finish with a R_a of 9.5 nm was achieved at 28.000 min^{-1}. The surface finish stays below R_a 20 nm for a very broad rotational speed band, only increasing significantly under 10.000 min^{-1}. The variance between the individual spindle speed settings is most likely caused by resonance. Figure 9 lists the surface roughness R_a as well as S_a for the experiment.

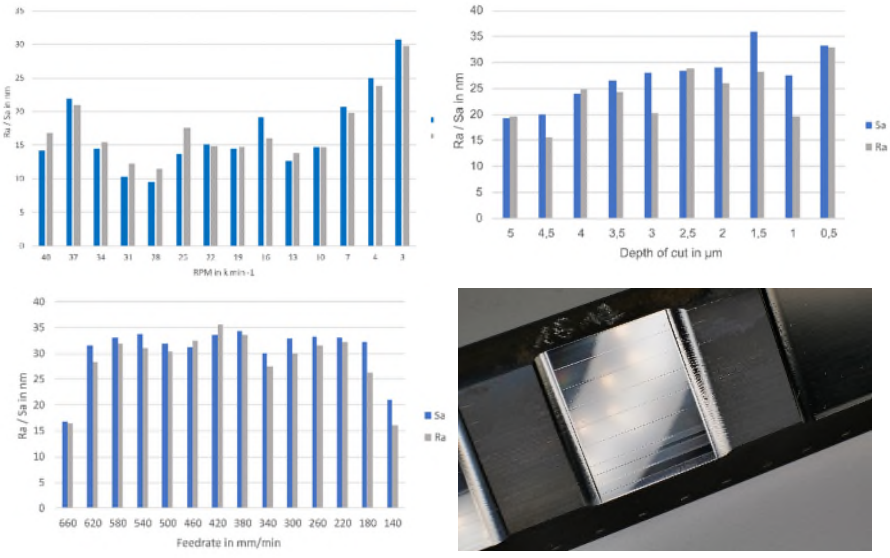

Figure 9: From top left, clockwise: Surface roughness for the spindle speed variation, feedrate variation, depth of cut variation. Picture of a finished specimen. The sample area division and gloss are easily recognizable.

The surface roughness does not significantly change with decreasing feedrate (see figure 10). The large change from 660 mm/min to 620 mm/min is most likely attributable to a break in period of the PCD-RB milling tool. Figure 10 shows an exemplary confocal laser scanning microscope (CLSM) picture of the surface. Varying the feedrate had no discernible impact on the surface roughness. The sample surface under the CLSM appear almost identical, similar to an optical inspection.

It can be seen that with decreasing depth of cut the surface roughness generally deteriorates (figure 10). At the lower values this is most likely because the pre-finishing operation is starting to show. The depth of cut has an influence on the gloss of the sample, with increasing DOC a higher gloss was visible.

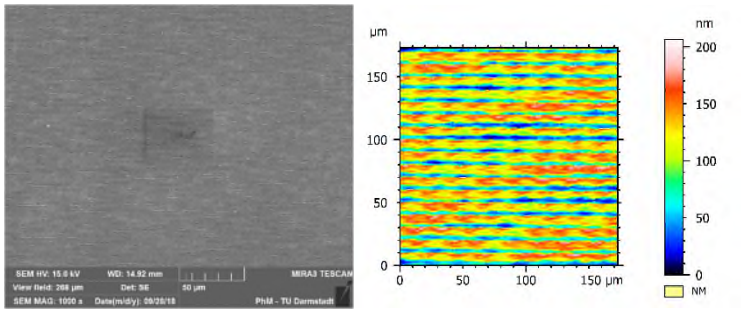

Figure 11: SEM and CLSM picture of the sample surface

Figure 11 shows a SEM picture of the surface after the finishing pass. Regular grooves in the feed direction are visible. Comparing their length and period with the process settings as well as referencing the likelihood of a particle becoming adhered to the tooling (see chapter 3), the groove surface fault mentioned in chapter 2 is identifiable as a picked up particle marring the surface.

5 Conclusion

The stainless steel used in the experiments (Stavax by Uddeholm) was analysed regarding its isotropy. First, a hardened specimen was manually polished. Indentation tests showed a hardness of 53 HRC, whereas the nanoindentation showed a steep increase in the surface hardness to a value of 7,5 GPa, which correlates to the normal indentation test. SEM pictures showed a clean, uniform surface with good polishing behaviour. BSE analysis suggests larger crystallographic grains and roughly one micrometre sized spherical inclusions of a lighter element, most likely carbon. This indicates a very uniform material after hardening. The surface faults visible in the milled sample specimen are therefore not related to the material, proofing Stavax to be an apt choice for the finishing process proposed in this paper.

A subjectively good surface quality is foremost defined by the gloss exhibited by the sample. It can be marred by the surface faults apparent, and the surface roughness is an easily measurable quality. Nevertheless, the challenge to combine these three factors into one process is difficult to achieve.
Spindle speed, feed, depth of cut and their influence on the surface roughness were evaluated. The spindle speed has no noticeable impact on the surface roughness. The surface roughness improves with a higher DOC, and a slower feedrate returns a better surface as well. A higher depth of cut also increases the gloss of the sample surface. A tool analysis in combination with the process variation showed that the grooves marring the surface are caused by small particles adhering to the tool. At higher rotational speeds, the occurrence decreased.

Because the polycrystalline diamond tool left a black, tough residue on the surface, the possibility of chemically cleaning the sample was regarded. A 2M solution of NaOH lye proofed to be very effective in cleaning the film. Washing the sample in distilled water as well as finishing the surface with methanol alcohol proofed to be a working and cost-effective solution to cleaning the surface. The surface roughness measurement was improved from 15 nm to 11 nm by the used approach.

6 Prospection

This paper has only evaluated one specific type of stainless steel. In mould making, besides ESR steels (of which Stavax is a good representative), powder metallurgic steels such as Elmax are very common, too. Because of the finer grain size, their polishing performance is often higher, enabling lower surface roughness. Moreover, a high surface finish in titanium, aluminium and other metals is sought after, suggesting a material study with the existing process.

References

[1] GVR. “Injection Molded Plastics Market Size Report By Raw Material (PP, ABS, HDPE, PS), By Application (Packaging, Consumables & Electronics, Automotive, Construction, Medical), And Segment Forecasts, 2018 - 2025”. In: Grand View Research (2018)
[2] S.J. Zhang et al. “A review of surface roughness generation in ultra-precision machining”. In: International Journal of Machine Tools and Manufacture 91 (2015), pp. 76–95.
[3] 3DHubs. SPI Mold Finish Standard. Internet Page.
[4] Julong Yuan et al. “Review on the progress of ultra-precision machining technologies”. In: Frontiers of Mechanical Engineering 12.2 (2017), pp. 158–180.
[5] Paul Morantz Paul Shore. “Ultra-precision: enabling our future.” In: Philosophical Transactions of the Royal Society No. 370 (2012), pp. 3993–4014.
[6] Tom Solon. “Fundamentals of ultraprecision machining”. In: Machine Design (2012).
[7] M. Azizur Rahman et al. “Variation of surface generation mechanisms in ultra-precision machining due to relative tool sharpness (RTS) and material properties”. In: International Journal of Machine Tools and Manufacture 115 (2017). Far East Innovations in super-fine finishing of complex optics, pp. 15–28.
[8] A. Simoneau, E. Ng, and M.A. Elbestawi. “Surface defects during microcutting”. In: International Journal of Machine Tools and Manufacture 46.12 (2006), pp. 1378–1387. [9] Norbert Mair. “Erzielbare Oberflächenqualitäten beim Planfräsen mit einstellbarem Diamantwerkzeug”. MA thesis. Hochschule Mittweida, 2011.